MORPHOLOGY, STRUCTURAL, AND SPECTRAL CHARACTERIZATIONS OF LAB-SYNTHESIZED MANGANESE OXIDES RELEVANT TO MARS.

Yanqing Xin[1, 2], Zongcheng Ling[1*], Haijun Cao[1], Changqing Liu[1], Hongchun Bai[1]. [1]Shandong Provincial Key Laboratory of Optical Astronomy and Solar-Terrestrial Environment, School of Space Science and Physics, Institute of Space Sciences, Shandong University, Weihai, Shandong, 264209, China. [2]Key Laboratory of Lunar and Deep Space Exploration, CAS. (zcling@sdu.edu.cn).

Introduction: Manganese is one of the important transition metals on Earth and Mars. On Earth, Mn is relatively abundant with an average upper crustal abundance of ~0.19 wt % MnO[1] while is ~0.4 wt % in basalts on Mars [2]. The Mn is a redox-sensitive element and has several oxidation states, such as +2, +3, +4, +6, and +7. On those Mn oxidation states, Mn^{2+} is soluble, with Mn^{3+} and Mn^{4+} forming minerals in the form of Mn_2O_3 and MnO_2 precipitation. Therefore, Mn is an important indicator of planetary mineral and geologic evolution because its valence change is more complex.

Mars rovers Curiosity and Opportunity have found Mn-rich minerals in multiple sedimentary outcrops at Gale and Endeavour Crater, respectively [3,4], but the exact mineral species still need to be confirmed. In the Kimberley region at Gale Crater, the content of Mn of fracture-filling materials that crosscut sandstone was found to be higher than 25%, indicating the existence of Mn-oxides rather than evaporites or other salts [5]. Furthermore, hydrated Mn-oxides were also found in Martian breccia meteorites NWA 7034 and NWA 7533. Those phases contain Mn contents up to ~32% and experimental studies show that the Mn-oxide minerals are Mn(IV)-oxides, but it is hard to identify the mineral species (birnessite or vernadite) due to its fine grain size and the aggregate nature [6].

In this work, we focus on the laboratory spectroscopic studies of seven pure Mn-oxides (α-, β-, γ-, δ-MnO_2, α-Mn_2O_3, α-Mn_3O_4, γ-MnOOH). They were synthesized with hydrothermal reaction and solid-state calcination methods, using SEM, EDS to get their morphology and chemical composition, XRD to the identification of Mn-oxides. Then the spectroscopy technique such as Raman was used to characterize their spectral characteristics.

Samples Preparation: Five Mn-oxides (α-, β-, γ-, δ-MnO_2, γ-MnOOH) were synthesized by hydrothermal reaction through a Teflon-lined stainless steel autoclave at different temperatures ranging from 90 to 150 ℃. The two other Mn-oxides (α-Mn_2O_3 , α-Mn_3O_4) were synthesized by solid-state calcination methods using a muffle furnace in the air at 600 ℃ , 1000 ℃, respectively. The initial reagents were $MnCl_2$, $MnSO_4$, $KMnO_4$, $(NH_4)_2S_2O_8$, $Mn(CH_3COO)_2$, $MnCO_3$, etc. Detailed information on the sample synthesis is listed in Table 1.

Sample Characterization: The SEM (Nano SEM 450, USA) and EDS (Aztec Xmax 50, UK) were employed to check the morphology and chemical compositions of Mn-oxides. XRD patterns of Mn-oxides synthesis in the laboratory were collected on an X-ray diffractometer (Rigaku UltimaIV, Japan). The Raman spectra of the synthesized Mn-oxides were collected by inVia Raman System (Renishaw, UK). All the above experiments were conducted at Shandong University at Weihai.

Table 1 Synthesis conditions

synthesis method	objective minerals	reagents	temperature	time duration	dry temperature
hydrothermal reaction	α-MnO_2	$MnSO_4$ $KMnO_4$	150℃	24h	60℃
	β-MnO_2	$MnSO_4$ $(NH_4)_2S_2O_8$	140℃	12h	100℃, calcination @ 400℃
	γ-MnO_2	$MnCl_2$ $(NH_4)_2S_2O_8$	90℃	24h	60℃
	δ-MnO_2	$MnSO_4$ $KMnO_4$	140℃	2h	80℃
	γ-MnOOH	$Mn(CH_3COO)_2$ $KMnO_4$	150℃	72h	85℃
solid-state calcination	α-Mn_2O_3	$MnCO_3$	600℃	5h	
	α-Mn_3O_4	$MnSO_4$	1000℃	17h	

Morphology and Chemical Compositions: The SEM images (Figure 1) show the synthesized Mn-oxides have different morphology. The α-MnO_2 presents nanofibrous forming an irregular ball with ~8 μm in diameter. β-MnO_2 was a nanorod with an average length of ~1.6 μm and has good crystallinity. γ-MnO_2 presents with small poorly nanosheets and nanorods mixing in clusters with a diameter range from ~1 to ~12 μm. δ-MnO_2 has a homogeneous nanosphere with ~400-~600 nm in diameter. α-Mn_2O_3 was presented with a nanosheet structure stacked to form a porous nanosphere with ~2 μm in diameter. Crystalline α-Mn_3O_4 with a hard dumbbell-like nanostructure. γ-MnOOH has presented nanorods with a length-range between ~20 to ~150 μm. All the above morphology shows that the α-Mn_3O_4, γ-MnOOH, α-Mn_2O_3 have good crystallinity compared with x-MnO_2 (x = α, β, γ, δ) synthesized at low temperature. EDS was employed to detect the chemistry of Mn-oxides. The results are listed in Table 2. The results reveal that the β-, γ-MnO_2, α-Mn_3O_4, γ-MnOOH, α-Mn_2O_3 are only composed of Mn and O without other elements. However, α-MnO_2 and δ-MnO_2 have K element in their chemical composition, which may be due to their tunnel or layered structures. Previous studies reported that the α-MnO_2 with (2×2) tunnel structure and the δ-MnO_2 with layer structure can accommodate ion (K, Na, Ca, Ba) or water molecule[7].

52nd Lunar and Planetary Science Conference 2021 (LPI Contrib. No. 2548)

1955.pdf

All the stoichiometric ratio of Mn-oxides are generally in accord with their nominal formula.

Phase Identification: The phase information of the Mn-oxides shows in Figure 2. The XRD patterns of those Mn-oxides are consistent with their PDF-2004 mineral database, indicating the purity of synthesized Mn-oxide phases. We calculated the FWHM (Full Width at Half Maxima) of their main peak. The results reveal that the α-Mn_3O_4 (FWHM=0.098°) and γ-MnOOH (FWHM=0.164°) have good crystallinity, while the δ-MnO_2 (FWHM=1.588°), α-MnO_2 (FWHM=0.825°), γ-MnO_2 (FWHM=0.653°) have poor crystallinity. This observation agrees well with morphology measurements by the SEM.
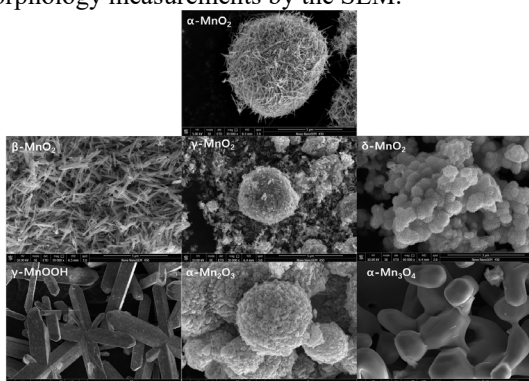

Figure 1 The Morphology of the Mn-oxides

Table 2 The Elements of Mn-oxides detected by EDS

Mn-oxides	Element	Average Atomic(%)
α-MnO_2	O	62.05
	K	3.75
	Mn	34.2
β-MnO_2	O	62.68
	Mn	37.32
γ-MnO_2	O	62.12
	Mn	37.88
δ-MnO_2	O	55.54
	K	8.03
	Mn	36.43
α-Mn_2O_3	O	50.64
	Mn	49.36
α-Mn_3O_4	O	42.68
	Mn	57.32
γ-MnOOH	O	63.18
	Mn	36.82

Raman Spectra Studies: As shown in Figure 3, the seven Mn-oxides exhibit distinct individual peaks in their Raman spectra, which can be used as fingerprint spectra for phase identification. Generally, the range of the spectra of Mn-oxides can be divided into two parts, ~100-400 cm^{-1}, ~400-750 cm^{-1}. In the range of 500-700 cm^{-1}, the Raman spectra can be used to distinguish the MnO_2 from other Mn-oxides such as γ-MnOOH, α-Mn_3O_4, and α-Mn_2O_3. All the Raman spectra of MnO_2 minerals exhibit major double peaks at ~570 and ~650 cm^{-1}. α-Mn_2O_3 shows double peaks at ~654 and ~702 cm^{-1}, while α-Mn_3O_4 has a single peak at ~660 cm^{-1}. γ-MnOOH has triple peaks at ~531, ~558, ~621 cm^{-1}. All those strong high wavenumber peaks are derived from the stretching mode of MnO_6 octahedra, making them of priority for discriminate those Mn-oxides. There are

also multiple low wavenumber peaks lower than ~400 cm^{-1}, originating from the bending mode of MnO_6 octahedra.
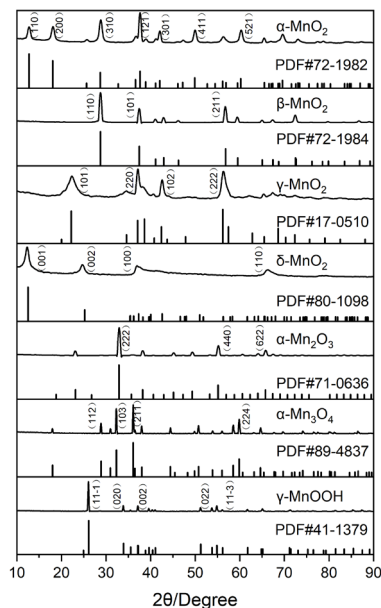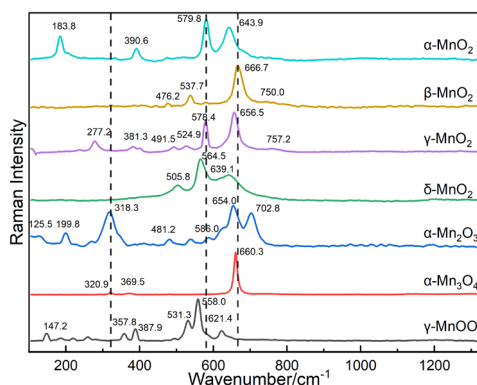

Figure 2 The XRD patterns of the Mn-oxides

Figure 3 The Raman spectra of Mn-oxides

Conclusion: This work provides detailed morphology, structural, spectroscopic studies of seven Mn-Oxides synthesized in the laboratory. Future work will extend to other spectroscopic studies such as MIR and VINR. These experimental characterizations show that the Raman spectroscopy is powerful to straight-forward identify the seven Mn-oxides. It gives a promising technique to employ the datasets acquired by future Raman instruments selected for Mars missions, i.e., SuperCam and SHERLOC on Perseverance rover and RLS on ExoMars.

References: [1] Turekian K. K. et al. (1961) *Geol. Soc. Am. Bull., 72,* 175. [2] McSween H. Y. et al. (2004) *Science, 305,* 842. [3] Arvidson R. E. et al. (2016) *Am., 101,* 1389. [4] Lanza N. L. et al. (2014) *Geophys. Res. Lett, 41,* 5755.[5] Lanza N. L. (2016) Geophys. Res. Lett., 43, 7398. [6] Liu Y. et al. (2017) *LPSC, LPICo No. 1964.* [7] Post J. E. et al. (2020) *Am.., 105,* 1175. [7] Irvine T. N. et al. (1971) *J. Earth Sci., 8,* 523-548. [8] Anderson R. et al. (2015) *Icarus, 249,* 2-21.